

SCIENTIFIC REPORTS



OPEN

ZipN is an essential FtsZ membrane tether and contributes to the septal localization of SepJ in the filamentous cyanobacterium *Anabaena*

Sergio Camargo¹, Silvia Picossi¹, Laura Corrales-Guerrero², Ana Valladares¹, Sergio Arévalo¹ & Antonia Herrero¹

The organismic unit of heterocyst-forming cyanobacteria is a filament of communicating cells connected by septal junctions, proteinaceous structures bridging the cytoplasm of contiguous cells. This distinct bacterial organization is preserved during cell division. In *Anabaena*, deletion of the *zipN* gene could not be segregated. We generated strain CSL109 that expresses *zipN* from a synthetic regulatable promoter. Under conditions of ZipN depletion, cells progressively enlarged, reflecting restricted cell division, and showed drastic morphological alterations including cell detachment from the filaments, to finish lysing. In contrast to the wild-type localization in midcell Z-rings, FtsZ was found in delocalized aggregates in strain CSL109. Consistently, the proportion of membrane-associated to soluble FtsZ in fractionated cell extracts was lower in CSL109. Bacterial two-hybrid analysis showed that ZipN interacts with FtsZ and other cell-division proteins including cytoplasmic Ftn6 and SepF, and polytopic FtsW, FtsX, FtsQ and FtsI. Additionally, ZipN interacted with the septal protein SepJ, and in CSL109 depletion of ZipN was concomitant with a progressive loss of septal specificity of SepJ. Thus, in *Anabaena* ZipN represents an essential FtsZ membrane tether and an organizer of the divisome, and it contributes to the conformation of septal structures for filament integrity and intercellular communication.

Cyanobacteria are characterized by a phototrophic mode of life relying on oxygenic photosynthesis. Regarding nitrogen assimilation, simple compounds such as nitrate, ammonium, or urea are excellent nitrogen sources, and many strains are also able to fix atmospheric nitrogen. However, ammonium is a preferred nutrient so that, when available, it impedes the assimilation of alternative nitrogen sources¹. In filamentous heterocyst-forming strains, the organismic unit is a string of communicating cells that can include different cell types that exchange nutrients and regulatory molecules². Particularly, in the absence of combined nitrogen, some cells localized at semi-regular intervals along the filament differentiate into heterocysts, cells specialized in the fixation of atmospheric nitrogen. Thus, under these conditions the filament is composed of vegetative cells that perform oxygenic photosynthesis and fix CO₂, and heterocysts that fix N₂. The cells in the filament may communicate through a shared periplasm, which is delimited by the cellular inner membrane and an outer membrane that is continuous along the filament, and by proteinaceous channel structures that are located in the septal regions between neighbouring cells³. The polytopic protein SepJ is located at the cell poles and is required to form long filaments^{4,5} and to exhibit normal activity of intercellular molecular exchange⁶. Hence, SepJ has been considered to represent a structural component or organizer of septal complexes (known as septal junctions)^{3,7} that would expand the intercellular periplasmic regions providing cell-to-cell adhesion and communication throughout the filament^{7,8}. The cyanobacterial filament grows by intercalary cell division and reproduces by random trichome breakage, and in strains such as

¹Instituto de Bioquímica Vegetal y Fotosíntesis, Consejo Superior de Investigaciones Científicas and Universidad de Sevilla, Américo Vespucio 49, E-41092, Seville, Spain. ²Present address: Laboratory for Microbiology, Faculty of Biology, Philipps University, Marburg, Germany. Correspondence and requests for materials should be addressed to A.H. (email: herrero@ibvf.csic.es)

those of the genus *Anabaena* that produces unbranched filaments, the division plane is always perpendicular to the long filament axis⁹. This distinct biological organization must include cell division mechanisms different from those present in the more common bacteria producing separated daughter cells³.

In the vast majority of studied bacteria, cell division is initiated by the polymerization of the tubulin homolog FtsZ to form a ring at the future site of division. FtsZ has no membrane-interacting domain, but the Z-ring is bound to the cytoplasmic side of the inner membrane by a variety of protein tethers as found in different bacteria (e.g.^{10,11}), of which the FtsA and ZipA proteins are the best studied examples^{12–14}. The Z-ring serves as a scaffold for the recruitment of further protein components to form the divisome complex, which includes periplasmic domains and promotes peptidoglycan remodelling (to synthesize the polar caps of the daughter cells), chromosome segregation and membrane fission^{15,16}. In cyanobacteria, cell division has been studied mostly in unicellular strains, whereas in filamentous cyanobacteria the investigation of division mechanisms has been scarce, and the identification of components of the division machinery has mostly been based on protein sequence comparisons^{17,18}. It has been concluded that cyanobacteria generally have some divisome components in common to Gram-negative bacterial models, others in common to Gram-positive models, and still others found only in cyanobacteria and chloroplasts, photosynthetic organelles that are of cyanobacterial origin. Notably, cyanobacteria in general lack homologs of FtsA or ZipA. However, they generally bear homologs of SepF from Gram-positive bacteria, which in *Bacillus subtilis* has been shown to contribute to the correct arrangement of FtsZ filaments and represent an additional FtsZ tether^{10,19}.

In the rod-shaped unicellular cyanobacterium *Synechococcus elongatus* strain PCC 7942, filamentous mutants (single elongated cells reminiscent of the classical *fts* *Escherichia coli* mutants) that resulted from transposon mutagenesis led to the identification of the *ftn2* and *ftn6* genes, which have orthologues only in other cyanobacteria and in plant chloroplasts²⁰. Indeed, phylogenetic trees based on the sequences of Ftn2 (later known as ZipN) orthologues from strains representative of all the clades throughout the phylum cyanobacteria almost perfectly mirrored the reference trees for cyanobacterial phylogeny, suggesting that the gene encoding this protein was mainly vertically inherited through the phylum²¹. Regarding function, in the spherical unicellular cyanobacterium *Synechocystis* sp. strain PCC 6803, in which cell division proteins have been most extensively studied, ZipN is required for normal cytokinesis²². Because of its interaction with FtsZ and other essential divisome components, ZipN has been proposed to play a central role in divisome assembly similar to the *E. coli* cytokinetic factor FtsA²³. In the filamentous strain *Anabaena* sp. strain PCC 7120, an *ftn2* mutant exhibited enlarged cells and, similar to the situation in the unicellular spherical *Synechocystis* but in contrast to that in the unicellular rod-shaped *S. elongatus*, the mutation inactivating this gene could not be segregated²⁰. Notably, in *Anabaena* sp. strain PCC 7120 the septal protein SepJ has been shown to interact with the divisome during cell division²⁴.

In this work, we have addressed the role of ZipN in *Anabaena* sp. strain PCC 7120 (hereafter *Anabaena*), a model pluricellular filamentous cyanobacterium. By the study of the effects of ZipN depletion and ZipN interactions with other putative cell division factors, we found that ZipN is a principal FtsZ tether to the membrane and an essential organizer of the divisome. Moreover, ZipN contributes to the septal localization of SepJ, which is required for filament integrity and intercellular communication in the filament.

Results

The *zipN* gene and the ZipN protein of *Anabaena*. In the *Anabaena* genomic sequence, the *zipN* gene (*all2707*) is flanked by ORFs *alr2708*, which lies in the opposite orientation, and *all2706*, which starts 165 bp downstream from *zipN* in the same orientation (Fig. 1a). However, *all2706* appears to be transcribed independently of *zipN*. On the one hand, in global transcriptomic studies of *Anabaena*, a transcript discontinuity was found in the intergenic region between those genes²⁵, and a putative transcription start site was localized in this intergenic region²⁶. On the other hand, similar amounts of *all2706* transcripts were detected by semi-quantitative RT-PCR analysis with RNA isolated from *Anabaena* and strain CSL109 (Fig. 1d), the latter being altered in expression of *zipN* (see below). *zipN* encodes a 798-residue protein that was reported to include an N-terminal DnaJ domain (amino acids 6 to 70)²⁰. In *Synechocystis*, a corresponding sequence of ZipN is required for cell viability and ZipN interaction with FtsZ²². However, Arc6, the chloroplastic homolog of ZipN, has recently been classified as a DNAJ domain protein, which are proteins with so-called J-like domains that likely act as chaperons but in a manner independent of interaction with HSP70, as it is characteristic of the bona fide J-domain²⁷. Thus, the assignment of the N-terminal domain of cyanobacterial ZipN remains unclear. In addition, the *Anabaena* gene product includes a putative transmembrane helix (TMH) (residues ca. 608–630, as predicted by the following programs: SOSUI, TMHMM, constrained Phobius prediction, TMPred). The predicted topology for ZipN is however uncertain; thus, whereas some programs locate the N-terminus in the periplasm and the C-terminus in the cytoplasm (TMHMM; constrained Phobius prediction; TMPred), MEMSAT-SVM suggests the opposite orientation.

Generation of an *Anabaena* mutant altered in *zipN* gene expression. Given that previous attempts to generate an *Anabaena* derivative lacking *zipN* were unsuccessful²⁰, we intended the generation of mutants conditionally downregulated in *zipN* expression. The synthetic promoter P_{ND}, which is nitrogen-regulated and provides high expression levels in the absence of combined nitrogen or in the presence of nitrate and low levels in the presence of ammonium²⁴, was used. Strain CSL109 bears the construct P_{ND}-*zipN* preceded by gene-cassette C.S3, which includes transcriptional terminators in both orientations (Fig. 1a). As indicated by PCR analysis (Fig. 1b), in strain CSL109 this genomic structure is segregated, and no wild-type chromosomes could be detected. RT-qPCR analysis was performed with RNA isolated from filaments of the wild type and strain CSL109 grown with nitrate and incubated during five days in medium containing nitrate, ammonium or no combined nitrogen (diazotrophic growth). In the wild type, expression levels in the presence of nitrate or ammonium were about 0.7 and 0.6 times those in the absence of combined N, respectively. In CSL109, as expected from the regulation of the

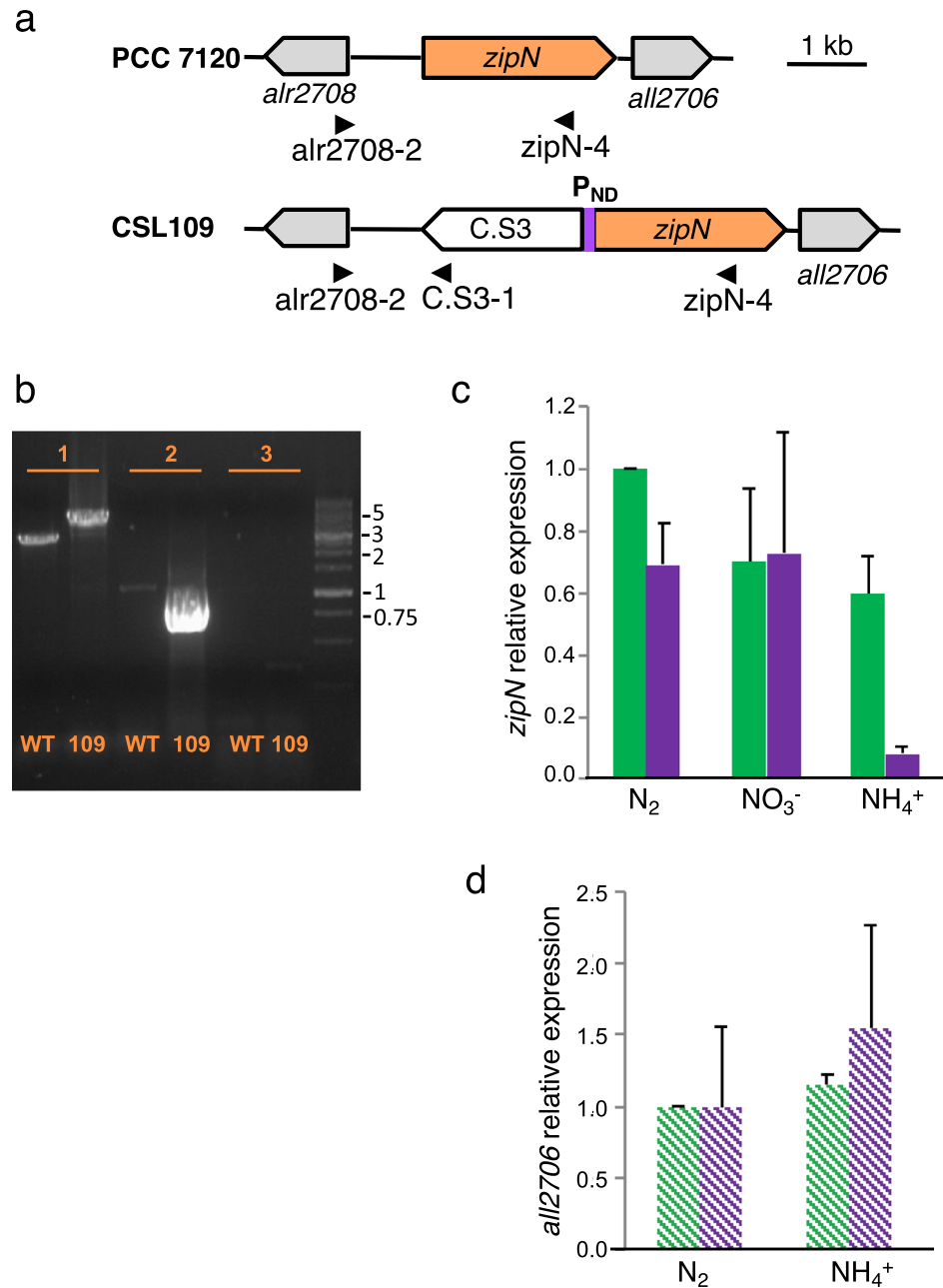


Figure 1. Genomic structure and *zipN* expression in strain CSL109. **(a)** Schematic of the *zipN* genomic region in strains PCC 7120 (WT) and CSL109, which expresses the *zipN* gene from a nitrogen-regulatable promoter (P_{ND}). C.S3 represents a gene-cassette providing Sm^R and Sp^R (see Materials and Methods for details). **(b)** Segregation of the P_{ND} -*zipN* construct in strain CSL109. PCR analysis was performed with DNA isolated from filaments of strains PCC 7120 (WT) and CSL109 (109) and the oligonucleotide pairs *alr2708-2/zipN-4* (1, expected sizes: 2,730 bp for the wild-type chromosomes and 4,830 bp for the mutant chromosomes generated by double recombination), *alr2708-2/C.S3-1* (2, expected sizes: 955 bp for the mutant and no band for wild type chromosomes) and *sacB1-sacB-2* (3, would produce a band of 1024 bp from the *sacB* gene only from chromosomes that would keep the transferred plasmid inserted by single recombination). Size markers (kb) are shown at right. The localization of the oligonucleotide primers is indicated with black arrowheads in **(a)**. **(c)** Levels of *zipN* transcripts in strains PCC 7120 and CSL109, relative to those of N_2 cultures of the wild type. RNA was isolated from BG11-grown filaments incubated 5 days under culture conditions in either BG11 (NO_3^-), BG11₀ (N_2) or BG11₀ plus ammonium (NH_4^+) medium, as indicated, and RT-qPCR was performed as described in Materials and Methods. Three to four independent cultures of each strain and incubation condition were used; error bars represent the standard error of the mean. Green bars, PCC 7120; purple bars, CSL109. **(d)** Levels of *all2706* transcripts in strains PCC 7120 and CSL109, relative to those of N_2 cultures of the wild type. RNA was isolated from BG11-grown filaments incubated 5 days under culture conditions, and semi-quantitative RT-PCR was performed as described in Materials and Methods. Two independent cultures of each incubation condition were used; error bars represent the standard error of the mean. PCC 7120, green; CSL109, purple.

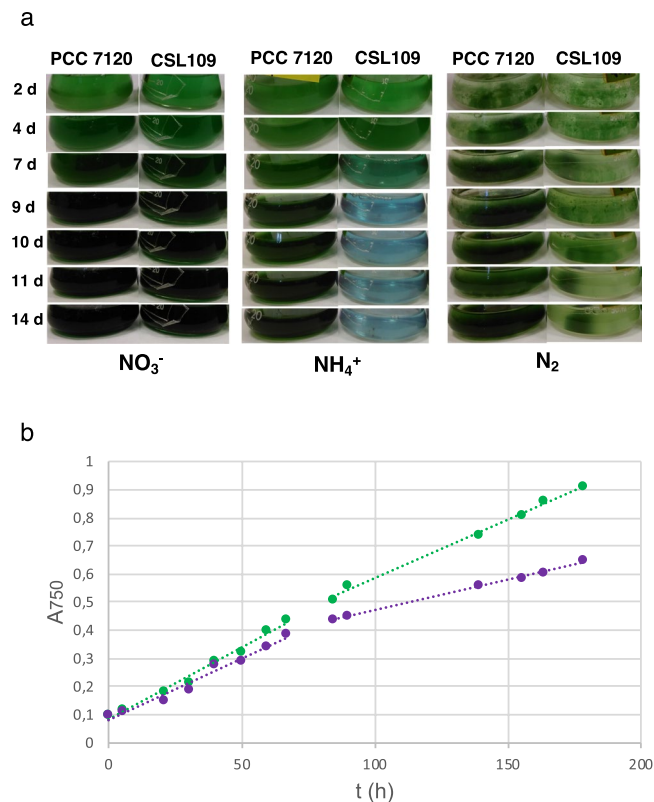


Figure 2. Growth of strain CSL109. Filaments of strain CSL109 ($P_{\text{ND}}\text{-zipN}$), and PCC 7120, grown in BG11 medium were collected and transferred to BG11 (NO_3^-), BG11₀ (N_2) or BG11₀ plus ammonium (NH_4^+) medium, at a cell density corresponding to 0.5 μg chlorophyll/ml, and incubation was continued under culture conditions. (a) Cultures were photographed after the indicated times (days) of incubation. Bluish color in strain CSL109 culture is indicative of cell lysis. (b) Absorbance at 750 nm was measured at the indicated times upon inoculation in BG11₀ plus ammonium (NH_4^+) medium of filaments of strain PCC 7120 (green) and CSL109 (purple). Note that in strain CSL109, increase in cell size with regard to the WT would contribute to increase in turbidity.

P_{ND} promoter, expression levels were similar in BG11 and BG11₀ medium and about ten times lower in the presence of ammonium (Fig. 1c). Thus, strain CSL109 incubated with ammonium appears to be suitable for analysis of the cellular effects of ZipN depletion.

Growth and morphology of strain CSL109. In the presence of nitrate, strain CSL109 grew similarly to wild-type *Anabaena* (Fig. 2a). Under this condition, the cells of CSL109 appeared slightly bigger and elongated in comparison to the wild-type cells (Fig. 3). In the absence of combined nitrogen (N_2), CSL109 could form heterocysts (Fig. 3) and was able to grow, although impaired with regard to the wild type (Fig. 2a); the cells of CSL109 were somewhat smaller, but appeared similar in shape to the wild type cells (Fig. 3). When nitrate-grown filaments were transferred to medium containing ammonium, growth of strain CSL109 promptly decline with extensive cell lysis taking place after prolonged incubation under this condition (Fig. 2). Regarding morphology, a progressive increase in cell size was observed concomitantly with drastic changes in cell shape. Under these restrictive conditions for *zipN* expression, cells first elongated and later enlarged, leading to very aberrant giant cells detached from filaments (Fig. 3) that finally lysed (Fig. 2a). Detailed measurements of cell size showed that after 5 days of incubation the mean cell area of CSL109 with regard to the wild type was 1.2 fold in BG11, 0.8 fold in BG11₀, and 3 fold in the presence of ammonium (Fig. 4).

Finally, combined staining with FM1-43 (cytoplasmic and outer membrane) and DAPI (nucleoids) showed that after 5 days of incubation in the presence of ammonium most cells of strain CSL109 contained DNA (Fig. 5). The extensive distribution of DNA in the big cells of this strain suggests that, at least up to this stage, chromosome duplication was unimpaired.

Localization of FtsZ in filaments depleted of ZipN. The distribution of FtsZ between soluble and membrane fractions from wild-type *Anabaena* and strain CSL109 was studied by western blot of fractionated cell extracts using anti-FtsZ antibodies. As a control, antibodies against the photosystem II D1 (PsbA) protein, which is exclusively localized at membranes, were used. Extracts were prepared from cultures of filaments incubated with ammonium for 4 days. After estimation of the total content of FtsZ protein in the soluble and membrane fractions obtained from a given volume of culture, the ratio of FtsZ content in the former versus the later was calculated (Fig. 6 shows a representative experiment). In the wild type, the amount of soluble FtsZ was higher than

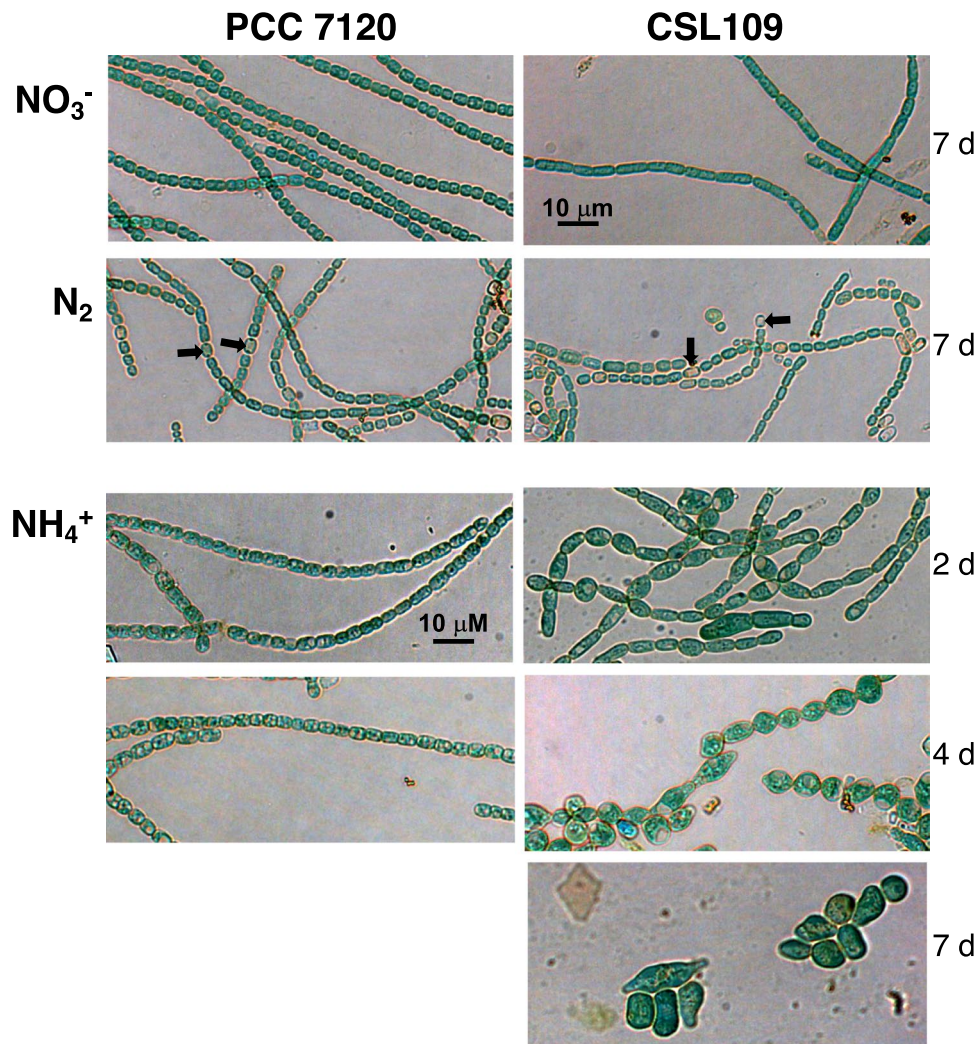


Figure 3. Morphology of strain CSL109. Filaments of strain PCC 7120 (WT) and CSL109 (P_{ND} -*zipN*) grown in BG11 medium (NO_3^-) were collected and transferred to BG11, BG11₀ (N_2) or BG11₀ plus ammonium (NH_4^+) medium, in which they were incubated for the indicated number of days under culture conditions. Samples of the cell suspensions were directly observed under a light microscope and photographed. Black arrows in N_2 point to some heterocysts. Magnification was the same for all micrographs.

the amount recovered associated to membranes, and this ratio was much higher for strain CSL109 (soluble FtsZ was 10.6- and 84.8-fold higher than the membrane-associated FtsZ for the WT and CSL109, respectively; mean of two determinations with similar results).

We also studied the localization of FtsZ by immunofluorescence with anti-FtsZ antibodies in strain CSL109 and compared it to the wild type. After transfer of nitrate-grown filaments to medium containing ammonium, many cells of the wild type presented FtsZ rings located at midcell. In contrast, in the bigger cells of CSL109 FtsZ was mostly found dispersed throughout the cell, including some delocalized foci and filament-like structures (Fig. 7a).

Finally, a version of the *Anabaena ftsZ* gene transcriptionally fused to *gfp-mut2* was transferred to strain CSL109 and, as a reference, to the wild type. The resulting strains, CSS86 and CSS85, respectively, bear the *ftsZ-gfp* gene construct inserted in the *ftsZ* region next to the native *ftsZ* gene (Fig. 7b, upper part). In both strains the fusion gene is expressed from the native *ftsZ* gene promoter. The localization of GFP fluorescence was studied in filaments of strain CSS86 and, for comparison, of strain CSS85 after transfer to ammonium-containing medium. Figure 7b, lower part, shows representative images and demographic representations of the localization of GFP fluorescence with regard to midcell over hundreds of cells of CSS85 and CSS86. In strain CSS85, GFP fluorescence was frequently detected in ring-like structures located at midcell. Accordingly, demographic representation showed a clearly preferred distribution around midcell. In CSS86 fluorescence frequently appeared in delocalized patches or forming aberrant filament-like structures either oriented parallelly with regard to the longer cell axis or perpendicular and eccentric, consistent with a disperse localization in the demograph. Taken together, results described in this section indicate that a sufficient level of ZipN is required for the correct localization of FtsZ in membrane-anchored Z-rings located at midcell.

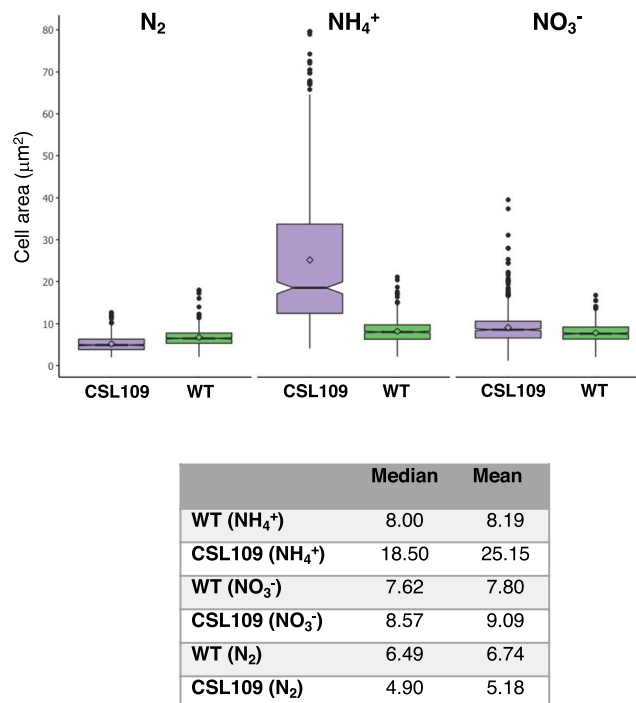


Figure 4. Cell area in strain CSL109. Filaments of *Anabaena* (WT; green) and strain CSL109 (P_{ND}-zipN; purple) grown in BG11 medium were collected and transferred to BG11 (NO₃⁻), BG11₀ (N₂) or BG11₀ plus ammonium (NH₄⁺) medium, in which they were incubated under culture conditions. After 5 days, samples of the cell suspensions were withdrawn and used for cell area determination. 500–600 cells from four different cultures were measured for each strain and culture condition. A box plot representation of the data is shown. The table summarizes the values of the median and the mean. Tukey's HSD (honest significant difference) and U Mann Whitney tests were performed to assess the statistical significance of comparisons. Both parameters were 0.000 for comparisons between strains PCC 7120 and CSL109 with NH₄⁺ or N₂, and were 0.000 (U Mann Whitney tests) and 0.006 (Tukey's HSD) with NO₃⁻ (in all cases lower than 0.05, thus meaning significant differences). Also, both parameters were 0.000 for comparisons of CSL109 with different nitrogen sources, again meaning significant differences.

BACTH analysis of ZipN interactions. To get further insight into the role of ZipN in *Anabaena*, its ability to interact with other proteins involved in cell division was tested by bacterial two hybrid assays based on the reconstitution of adenylate cyclase from *Bordetella pertussis*. The tested partners included the *Anabaena* cell division proteins FtsZ, Ftn6 (also known as ZipS) and FtsI, and orthologues of SepF (Alr0487), FtsW (All0154), FtsE (Alr1706), FtsX (All1757) and FtsQ (Alr3857). Besides those, interaction was tested with the septal protein SepJ. The predicted topology of the protein fusions tested is represented in Fig. 8. With ZipN only the version T25-ZipN could be cloned, and some fusions of the other partners could not be cloned either. The results of the β-galactosidase activity exhibited by the *E. coli* clones expressing T25-ZipN, or as a control the empty pKT25 plasmid, together with the indicated fusion protein, or the empty pUT18 or pUT18C plasmid, are presented in Fig. 9. Positive interactions of T25-ZipN with T18-FtsZ, FtsZ-T18, T18-FtsW, FtsX-T18, T18-FtsI, and T18-FtsQ, and very strong interactions with Ftn6-T18, SepF-T18, T18-SepF and SepJ-T18 were detected. No significant interaction was detected between T25-ZipN and T18-FtsE or T18-FtsX.

Localization of SepJ in strain CSL109. Given the strong interaction of ZipN with SepJ in BACTH analysis, we studied the localization of SepJ under conditions of ZipN depletion. First, we performed immunolocalization with SepJ antibodies in strain CSL109 and, as a reference, in the wild type incubated with ammonium. Under these conditions, the wild type presented SepJ well focused at the center of the septal regions between neighboring cells, as described previously²⁴. In strain CSL109 SepJ was detected focused in some septa, but it was also found in delocalized foci or patches in the cells (Fig. 10a).

In addition, the localization of SepJ was studied with GFP-fusions. For that, a gene construct including a *sepJ* gene 3' fused to *gfp-mut2* was transferred to strain CSL109 and, as a reference, to the wild type. In both cases the construct was inserted by single recombination in the *sepJ* region, generating strains CSS90 and CSS89, respectively, both of which express the fusion gene from the native *sepJ* gene promoter (Fig. 10b, upper part). GFP fluorescence was monitored by confocal microscopy in strains CSS89 and CSS90. When incubated in media containing either nitrate or no combined nitrogen, both strains showed fluorescence signals focused in the center of the intercellular septa, and in structures similar to a Z-ring in dividing cells (not shown), as described previously

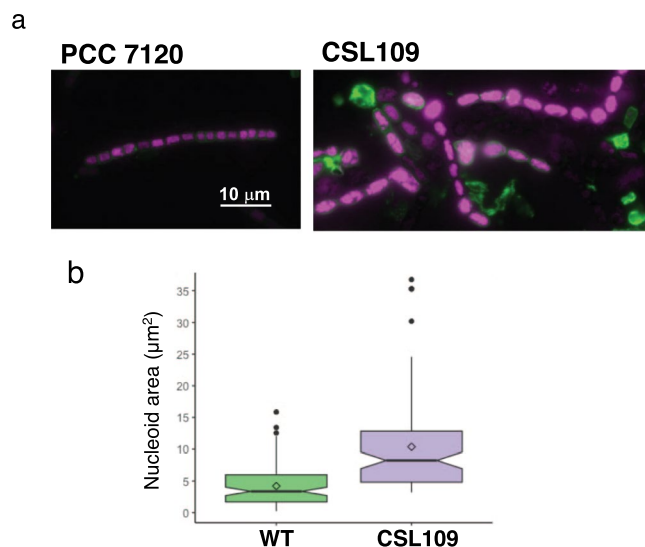


Figure 5. FM1-43 staining of the cytoplasmic and outer membranes and DAPI staining of nucleoids in strain CSL109. **(a)** Filaments of strains PCC 7120 (WT) and CSL109 (P_{ND} -*zipN*) grown in BG11 medium were incubated for 5 days under culture conditions in BG11₀ plus ammonium medium, stained with FM1-43 (green) and DAPI (magenta) dyes and photographed under a fluorescence microscope. Merged images of FM-43 and DAPI staining are shown. Magnification was the same for both micrographs. **(b)** DAPI images were used for nucleoid area determination. 106 cells of the WT and 96 of CSL109 were used. A box plot representation of the data is shown. The mean values (diamonds in the plots) were: WT, 4.2 μm^2 ; CSL109, 10.4 μm^2 .

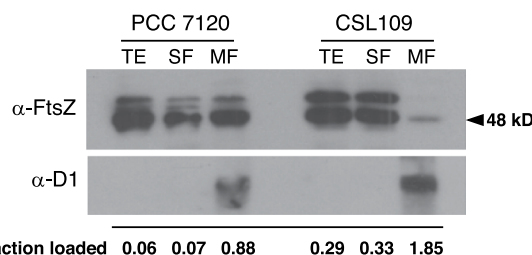


Figure 6. Western blot analysis of FtsZ distribution between soluble and membrane fractions. BG11-grown filaments of the indicated strains incubated for 4 days in BG11₀ plus ammonium medium were used to prepare cell-free extracts, which were fractionated as described under Materials and Methods. Aliquots of the extract obtained before fractionation (TE) and of the soluble (SF) and membrane (MF) fractions obtained after fractionation were loaded into 12% SDS/PAGE gels, electrophoresed and probed with antibodies raised against the *Anabaena* FtsZ protein²⁴ (upper panel). (The aliquots loaded account for the indicated percentage of the total amount obtained of the corresponding fraction). As a control of the purity of the fractions, hybridization was also performed with an antibody against the membrane protein D1 (lower panel). The total FtsZ amount present in the whole SF and MF was estimated after scanning and quantification of the gel bands. (As indicated by the use of *Anabaena* derivatives depleted of FtsZ, the three bands shown in the upper panel are produced by FtsZ²¹). Size indicator is shown at the right (predicted MW of FtsZ, 44.73 kDa).

for SepJ-GFP fusions in *Anabaena*⁴. When nitrate-grown cells were incubated in the presence of ammonium, strain CSS89 maintained the same GFP localization pattern as in BG11 or BG11₀ medium (Fig. 10b, lower part). In contrast, in strain CSS90, besides the intercellular spots (likely corresponding to structures already present in the filament before the transfer to ammonium-containing medium), additional fluorescence was detected in dispersed foci and in the periphery of enlarged cells (Fig. 10b, lower part). Taking together results of immunofluorescence and GFP-fusions, depletion of ZipN (in strain CSL109) appears to result in a substantial degree of SepJ delocalization as compared to the pattern observed in the presence of normal ZipN levels (in the wild type).

Discussion

The product of the *Anabaena* ORF *all2707* is ZipN, a cyanobacterial cell division factor. An unsegregated strain with inactivated *zipN* was reported to form elongated cells²⁰. We have now generated strain CSL109 that conditionally expresses *zipN* in response to the nitrogen source available in the external medium. In the presence of ammonium, expression of the gene in strain CSL109 is much lower than in the wild type and, under this condition, strain CSL109 shows a drastic increase in cell size concomitant with changes in cell shape. In contrast to the

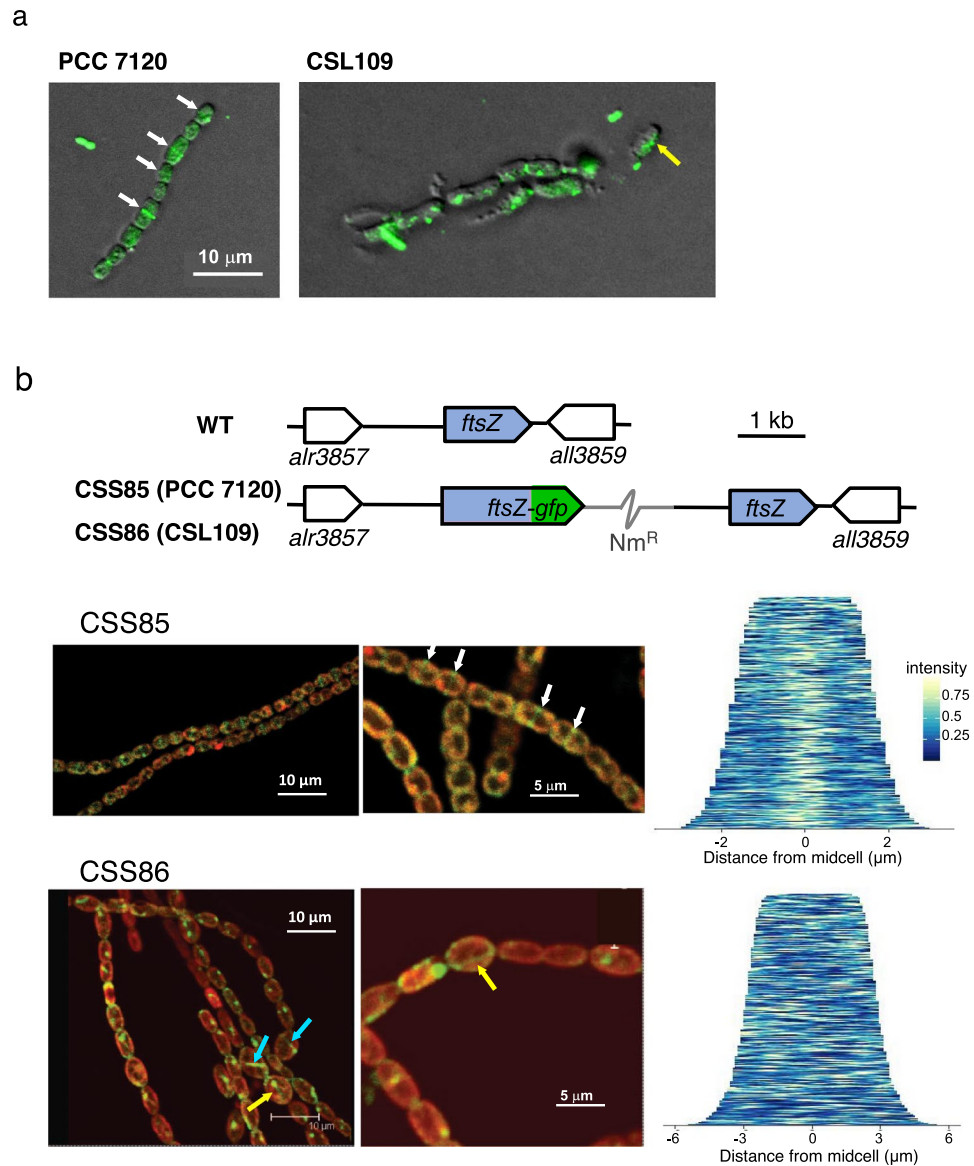


Figure 7. Localization of FtsZ in strain CSL109 depleted of ZipN. **(a)** BG11-grown filaments of strains PCC 7120 (WT) and CSL109 (P_{ND} -*zipN*) were incubated during 2 days under culture conditions in BG11₀ plus ammonium medium and then prepared for immunofluorescence with anti-*Anabaena* FtsZ-protein antibodies and visualized by fluorescence microscopy. Merged bright-field and immunofluorescence images are shown. White arrows point to apparent midcell FtsZ rings, and yellow arrow to an aberrant filament-like structure. Magnification was the same for both micrographs. **(b)** Genomic structure of the *ftsZ* genomic region in strain PCC 7120 (WT, native region) and in the strains CSS85 and CSS86, expressing an FtsZ protein C-terminally fused to mut2-GFP in the PCC 7120 and the CSL109 background, respectively. Nm^R represents a Nm-resistance genetic determinant included in the plasmid inserted in the chromosome (grey trace) (see Materials and Methods for details) (upper part of the figure). Representative filaments of strains CSS85 and CSS86 incubated for 2 days in BG11₀ plus ammonium medium were visualized by confocal microscopy. Merged images of cyanobacterial autofluorescence (red) and GFP fluorescence (green) are shown in the lower part of the figure. White arrows point to midcell FtsZ rings. Some aberrant filament-like structures parallel (yellow arrows) or perpendicular (blue arrows) to the longer cell axis are also indicated. Demographic representations of the distribution of GFP fluorescence with regard to midcell over 276 cells of CSS85 and 324 cells of CSS86 are also shown.

rod-shaped morphology of wild-type *Anabaena*, when strain CSL109 is transferred to conditions restrictive for *zipN* expression, cells first elongated and rounded, still forming filaments. Later, giant cells with irregular shapes are found, which were progressively detached from filaments and lysed. While the size increase indicates impairment in cell division, confirming ZipN as an essential cell division factor in *Anabaena*, the morphological changes and cell lysis suggest a discoordination between cell growth and lateral growth, with the latter becoming unable to follow the increase in cell size. Indeed, the morphology of strain CSL109 depleted of ZipN resembles that of

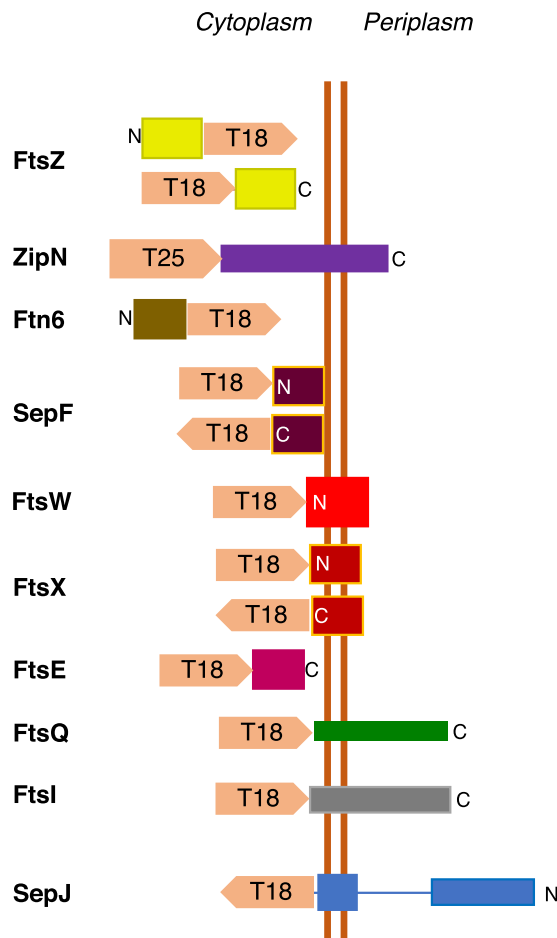


Figure 8. Schematic of the predicted topology of the protein fusions used in BACTH analysis. The T25 and T18 fragments of the catalytic subunit of adenylate cyclase are represented as block arrows indicating the orientation (N-terminal to C-terminal) of the polypeptide. FtsZ (428 amino acid residues), Ftn6 (227 amino acid residues) and FtsE (218 amino acid residues) are cytoplasmic proteins. ZipN (798 amino acid residues) has a TMH (residues ca. 608–630). SepF (198 amino acid residues) is a cytoplasmic protein predicted (Amphipaseek)³⁷ to have an N-terminal amphipathic membrane-anchor helix. FtsX (300 amino acid residues) is predicted to have four TMHs. FtsW (396 amino acids) is predicted to have eight TMHs, FtsQ (281 amino acid residues) is predicted to contain an N-terminal TMH. FtsI (609 amino acid residues) is predicted to have a TMH (amino acids 48–70). SepJ (751 amino acid residues) is predicted to have 11 C-terminal TMHs, with periplasmic linker and coiled-coil domains. N and C denote the N-terminus and the C-terminus, respectively.

the ovoid bacterium *Streptococcus pneumoniae*, in which depletion of the essential FtsZ tether FtsA results in cell ballooning and lysis²⁸. This has led to the proposal that, in contrast to the model bacilli *E. coli* and *B. subtilis*, in which FtsZ and FtsA direct septal but not peripheral peptidoglycan synthesis, in *Streptococcus* these proteins would coordinate both modes of peptidoglycan synthesis. Our results suggest that in *Anabaena* ZipN influences not only septal, but also lateral growth.

In the case of the spherical unicellular cyanobacterium *Synechocystis*, it has been suggested that ZipN is a functional analogue of the *E. coli* FtsA factor²³. However, to the best of our knowledge, it has not been previously shown for any cyanobacterium that ZipN is essential for FtsZ tethering to the membrane and FtsZ localization in midcell Z-rings. By means of both immunolocalization and GFP fusions, we have observed that in CSL109 cells depleted of ZipN, FtsZ appears in delocalized patches or in filament-like structures that are arranged parallelly or transversally with regard to the long filament axis, and eccentric. This is in contrast to the localization in midcell rings in the wild type. Additionally, we have observed by western blot analysis that in strain CSL109 depleted of ZipN the proportion of FtsZ bound to membrane is much lower than in the wild type. However, a low amount of FtsZ is still found in membrane fractions of CSL109 (Fig. 6). It is possible that the basal levels of ZipN that would remain in the cells could promote the association of some FtsZ with the cytoplasmic membrane. Also, the *Anabaena* homolog to SepF could contribute to atypical localization of FtsZ to the membrane under conditions of ZipN depletion.

Anabaena ZipN is predicted to include a transmembrane helix in its C-terminal part (residues ca. 608–630; ZipN is 798 residues long). Whereas different topology predictions give inconsistent results, our results of BACTH analysis showing positive interactions with T25-ZipN strongly suggests a cytoplasmic localization of the

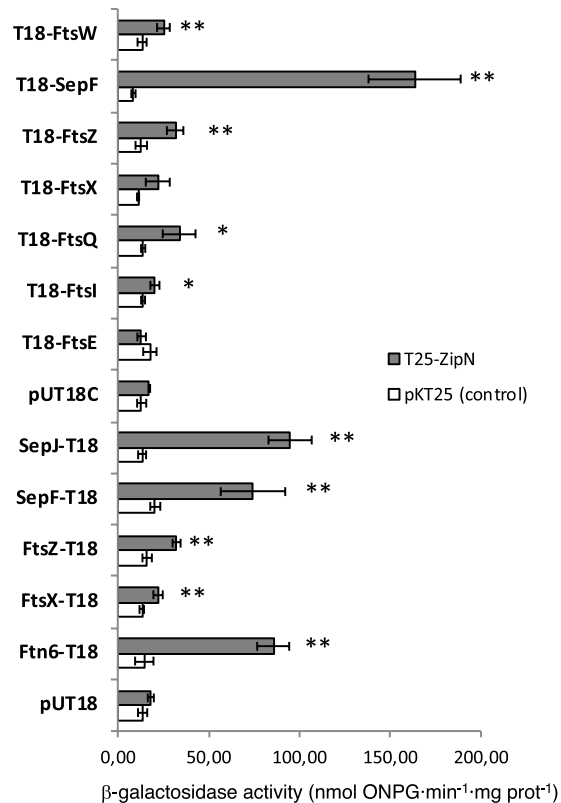


Figure 9. BACTH analysis of ZipN interactions. Interactions of proteins fused to T18 and T25-ZipN produced in *E. coli* were assayed by measurements of β -galactosidase activity in liquid cultures. The topology of each fusion is indicated by the order of components (T18-protein and T25-protein denotes the corresponding adenylate cyclase domain fused to the N-terminus of the tested protein; protein-T18 denotes the corresponding adenylate cyclase domain fused to the C-terminus of the tested protein). Data are the mean and SD of 3 to 10 determinations of the activity with T25-ZipN and the indicated fusion protein (or T25-ZipN and the corresponding empty vector pUT18 or pUT18C). Start symbols denote significant differences as assessed by Student's *t* tests (* $p < 0.05$; ** $p < 0.01$; values with regard to the two respective controls).

ZipN N-terminus since, to reconstitute an active enzyme, the two domains of adenylate cyclase should reside in the cytoplasm. Further on, the J-like domain (aa 6–70) of ZipN would also reside in the cytoplasm. Accordingly, T25-ZipN interaction with FtsZ has been detected in our assays. In summary, ZipN interacts with FtsZ and appears to be required for efficient FtsZ association to membranes and FtsZ localization in midcell rings, thus representing an essential determinant for FtsZ localization during cell division in *Anabaena*.

With regard to another cyanobacterial specific division factor, ZipS, its actual function has not been unraveled, although in unicellular cyanobacteria it has been related to the coordination of chromosome replication or segregation during cell division^{29,30}. Our results showing strong interactions of ZipN with the cytoplasmic proteins ZipS and SepF, besides FtsZ, suggest that in *Anabaena* the cytoplasmic domain of the Z-ring includes these four proteins. Furthermore, the ZipN interactions with the polytopic factors FtsW, FtsX, FtsQ, and FtsI suggest the participation of ZipN also in the conformation of the periplasmic part of the *Anabaena* divisome (Fig. 11). However, although statistically significant, these interactions are weak and should be further studied. (ZipN interaction with Ftn6 (ZipS), SepF, FtsQ and FtsI have also been detected with the *Synechocystis* proteins²³).

It has been previously reported that the septal protein SepJ that is involved in filament integrity and intercellular communication in *Anabaena* is recruited to the divisome and interacts with FtsQ, but not with FtsZ, during cell division²⁴. Here we have found a strong interaction of SepJ with ZipN, reinforcing the notion that during cell division SepJ is an integral component of the *Anabaena* divisome. Additionally, our study of the localization of SepJ in filaments of strain CSL109 showed a progressive loss of septal specificity of SepJ upon ZipN depletion. (The higher persistence of the SepJ signal at the cell poles observed with SepJ-GFP than by immunofluorescence could at least in part be due to increased stability of the fusion protein already located in the septa before the transfer to the ammonium-containing medium.) The disperse peripheral distribution of SepJ found after prolonged incubation in the presence of ammonium (Fig. 10b, see 3 days) suggests that, upon depletion of ZipN, SepJ can still interact with the cytoplasmic membrane but without the septal specificity found in the wild type. Taken together, the complementary results of two different approaches, namely the *in vivo* effects of ZipN depletion and BACTH analysis, suggest that ZipN-SepJ interactions contribute to the correct localization of SepJ in the intercellular regions of the filament. Furthermore, we have observed that upon depletion of ZipN in strain CSL109, cells progressively detach from the filament, resulting in separated aberrant cells (Fig. 3). Because inactivation of *sepJ* leads to a strong phenotype of filament fragmentation that, although stronger in the absence of combined

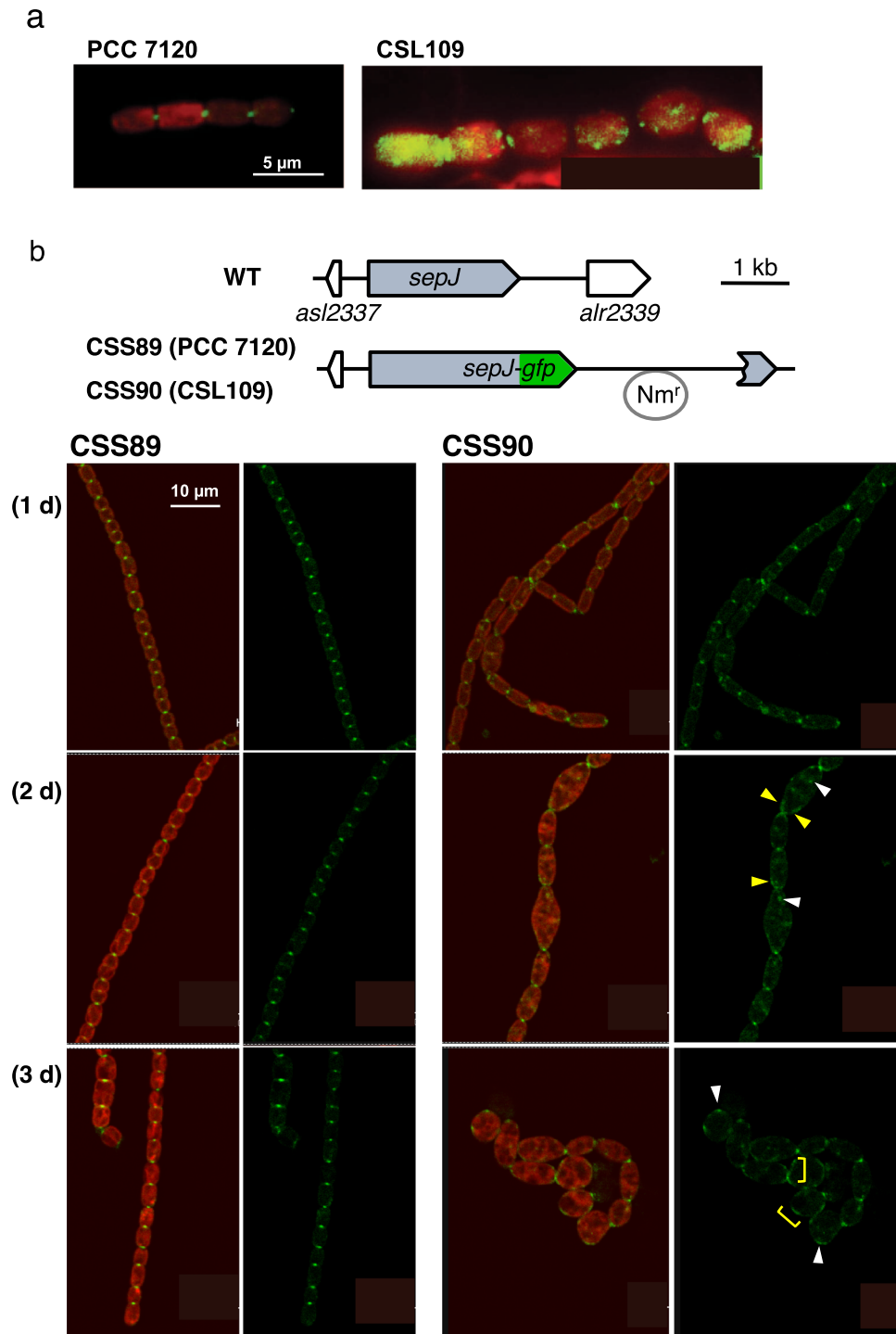


Figure 10. Localization of SepJ in strain CSL109 depleted of ZipN. **(a)** BG11-grown filaments of strains PCC 7120 (WT) and CSL109 (P_{ND} -*zipN*) were incubated during 2 days under culture conditions in BG11₀ plus ammonium medium and then prepared for immunofluorescence with anti-SepJ antibodies and visualized by fluorescence microscopy. Merged images of immunofluorescence (green) and cyanobacterial autofluorescence (red) are shown. Magnification was the same for both micrographs. **(b)** Localization of SepJ-GFP protein in cells depleted of ZipN. The genomic structure of the *sepJ* genomic region in strain PCC 7120 (WT, native region) and in the strains CSS89 and CSS90, expressing a SepJ protein C-terminally fused to GFP-mut2 in the PCC7120 and the CSL109 background, respectively, is shown in the upper part. Nm^R represents a Nm-resistance genetic determinant included in the plasmid inserted in the chromosome (grey trace) (see Materials and Methods for details). Representative filaments of strains CSS89 and CSS90 incubated during the indicated number of days in BG11₀ plus ammonium medium were visualized by confocal microscopy (lower part). GFP fluorescence (green) and merged images of cyanobacterial autofluorescence (red) and GFP fluorescence are shown. Some delocalized foci are signalled with white arrowheads, and some peripheral bands delocalized from the septa centre are indicated with yellow marks. Magnification was the same for all micrographs.

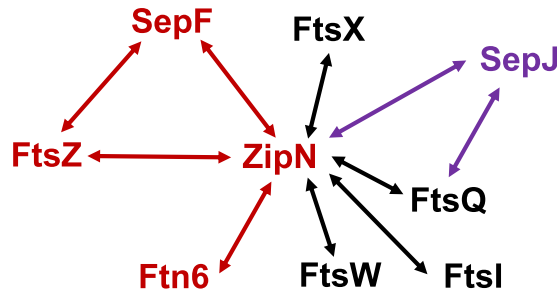


Figure 11. Model of a partial divisome of *Anabaena* based on ZipN and SepJ interactions. Interactions as deduced from BACTH assays are represented by arrows. The SepJ-FtsQ interaction was reported previously²⁴.

nitrogen, is also conspicuous in its presence⁴, impairment in septal localization of SepJ could contribute to cell detachment in CSL109. Thus, in addition to its essential role in the organization of the Z-ring and the divisome, ZipN appears to contribute during cell division to the conformation of septal structures that are necessary for filamentation and intercellular communication in *Anabaena*.

Materials and Methods

Strains and growth conditions. *Anabaena* sp. strain PCC 7120 and strain CSL109 were grown in BG11 medium (which contains NaNO₃ as a nitrogen source) containing ferric citrate instead of ferric ammonium citrate⁹. For incubation with other nitrogen sources, BG11₀ (containing no combined nitrogen) and BG11₀ plus ammonium (4–6 mM NH₄Cl and 8–12 mM TES-NaOH buffer, pH 7.5, instead of NaNO₃) medium were used. Cultures were incubated at 30 °C in the light (30 μmol photons m⁻² s⁻¹ from led lamps), in shaken liquid media or in plates in medium solidified with 1% Difco agar. For CSL109, media were supplemented with spectinomycin (Sp) and streptomycin (Sm) at 5 μg ml⁻¹ each in solid media or 2 μg ml⁻¹ each in liquid media; for CSS85 and CSS89, with neomycin (Nm) at 25 μg · ml⁻¹ in solid media or 5 μg · ml⁻¹ in liquid media; and for CSS86 and CSS90, with Sm, Sp and Nm at the concentrations indicated before.

Plasmid and strain constructions. To construct a strain that conditionally down-regulates *zipN*, plasmid pCSL131 was first generated. Two DNA fragments of the *zipN* region were amplified by PCR: fragment 1 comprises sequences upstream of *zipN* (amplified by PCR with primers alr2708-2/zipN-8; all oligodeoxynucleotide primers used are listed in Table 1); fragment 2 comprises sequences just upstream of and internal to the gene (amplified with primers zipN-9/zipN-10). Both fragments were inserted into plasmid pCSFR15, which includes the nitrogen-regulatable P_{ND} promoter preceded by gene-cassette C.S3²⁴, generating plasmid pCSL131. In this plasmid, fragment 1 is inserted (with ApaI/SalI ends) preceding the C.S3 sequence, and fragment 2 is inserted (with SacI/XhoI ends) following the P_{ND} sequence. Afterwards, the insert of pCSL131 was transferred, after digestion with ScaI restriction enzyme, to the mobilizable vector pCSBN1³¹, which includes a Nm^R determinant and the *sacB* gene (which determines sensitivity to sucrose), generating plasmid pCSL132, which was verified by sequencing. Plasmid pCSL132 was transferred by conjugation³² to strain PCC 7120 with selection for Sp^R and Sm^R. Cultures of Sp^R Sm^R exconjugants that had inserted the plasmid into the *zipN* locus by single crossover were used for selection of clones resistant to 5% sucrose which, by a second crossover event, should have inserted the C.S3-P_{ND} construct in front of the *zipN* gene. A clone that, according to PCR analysis (Fig. 1b), bore this construct in all chromosome copies was selected and named strain CSL109.

To express a FtsZ-GFP fusion, plasmid pCSS243 was constructed by transferring a *ftsZ-gfp* fusion from pCSC39 (Sm^R Sp^R)²¹ to pRL278 (Nm^R)³³, digesting both plasmids with SacI and BglII. Plasmids pCSS243 and pCSVT22 (which determines Nm^R and bears a *sepJ-gfp* fusion)³⁴ were transferred by conjugation to strains PCC 7120 and CSL109, as previously described³², selecting for Nm^R. The genetic structure of the selected clones was analysed by PCR (not shown). One clone resulting from each combination that bore the fusion gene in the corresponding genomic locus was selected. The resulting strains were named: CSS85 (*ftsZ-gfp* in wild-type background), CSS86 (*ftsZ-gfp* in CSL109 background) (see Fig. 7b), CSS89 (*sepJ-gfp* in wild-type background) and CSS90 (*sepJ-gfp* in CSL109 background) (see Fig. 10b).

Analysis of *zipN* and *all2706* expression. RNA was isolated from filaments of *Anabaena* strains grown in BG11 medium and incubated for 5 days in BG11, BG11₀ or BG11₀ plus ammonium medium (supplemented with antibiotics for the mutants). RNA (20 ng) was used for reverse transcription with the Quantitect Reverse Transcription kit (Qiagen). To study *zipN* gene expression, the obtained cDNA was used for real-time PCR as described²¹. The relative transcript levels of *zipN* are expressed as the ΔΔct value using genes *alr0599* and *all5167* (see²⁵) for normalization. The primer pairs used were: alr0599-1/alr0599-2 (*alr0599*), all5167-1/all5167-2 (*all5167*), zipN-15/zipN-16 (*zipN*), respectively.

To study *all2706* expression, semi-quantitative RT-PCR was performed with the same cDNA and the oligonucleotide primers all2706-3/all2706-4. The gene *alr0599* was used for normalization. The number of cycles at which the PCR reaction was in the exponential range was empirically determined. Samples were taken and resolved by electrophoresis in agarose gels, and the Image Lab software (Biorad) was used for quantification.

Preparation of *Anabaena* cell-free extracts and western blot analysis. Filaments suspended in PBS buffer (137 mM NaCl, 2.7 mM KCl, 10 mM Na₂HPO₄, 1.8 mM KH₂PO₄) supplemented with a protease

Name	Sequence (5'-3')
zipN-4	CTGATGAATACTGTGTCTCTGTT
zipN-8	AGACCAG <u>TCGACG</u> CCTTGTAACACCGTGCCA
zipN-9	ACAAGCGAGCTCTGGTCTAGGTGAATTATG
zipN-10	TAAAGTCTCGAGAGTACTGCTGGATGAATCGGA
zipN-15	CAACCCAGGGCAATTCTTACTC
zipN-16	CTGCCGATTACTTCTGATGGATG
zipN-21	AATAAACTGCAGTGATCACGGTGCAGG
zipN-22	CAAAAAGGTACCCTTAATTTATAGCGGCTGAC
alr0599-1	CCAATAGCTGGCCAGTGTTAGT
alr0599-2	GGAATTGCTTTGCCAGTTGTCAG
all5167-1	GCTCAAGCAATTCGTCACTGTTCC
all5167-2	AAAGATTGCGTCCGGTCTGGTGT
all2706-3	GCATCCACCAGCGATTGTAGAC
all2706-4	GGGTTGGTGATCGCACCAT
sacB-1	CTTGAGGTACAGCGAAGTG
sacB-2	TCTGCAAAAGGCCTGGAGG
C.S3-1	GGATGACCTTTGAATGACC
alr2708-2	AAGAAGGGGCCAGTACTGTGATTTTGGCGTTG
ftsZ-32	GTGAATTCCTTATTAATTTTGGGTGGTC
ftsZ-34	CCGAATCCCTGCAGACTTGATAATAAC
ftsZ-45	AAAACCGAATTCCTTTTGGGTGGTCGCGCTCTCT
ftsZ-46	GAATCCCTGCAGACTTGATAATAACCAAGAG
sepF-17	GACTAAGAATTCCTTATTGTGCCATCCGGT
sepF-18	TGCAACCTGCAGAACAAATATATTTCTAAAC
sepF-21	ATTTAAGAATTCCTGTGCCATCCGGTGGTTTC
all0154-11	GTAATGCTGCAGGAAGCTACGCAGCCTAATTC
all0154-13	ACTGTTGAATTCCTTAAACATCCGCCGACGTTG
all1616-1	AATATTCTGCAGACGATGGGTCGATGATTC
all1616-3	GTTGTTGAATTC AAGGAATTTTCGTTAGATATTGC
all1757-1	ATAGTGCTGCAGGTTTAAATTTCTCACGAACTTG
all1757-4	CACGCAGAATTC ACTA ACTTTTGGCAAAC
all1757-5	CGCATTGAATTCCTTACTTTTGGCAAACGTC
sepF-17	GACTAAGAATTCCTTATTGTGCCATCCGGT
sepF-18	GTGCAACTGCAGGAACAATATATTTCTAAAC
sepF-21	ATTTAAGAATTCCTGTGCCATCCGGTGGTTTC
alr0718-16	TAATAGCTGCAGGCAAAAGTCACCAAGTAG
alr0718-17	AACTTCGAATTCCTTAAGGTTTTCCTTCAATC
alr1706-4	TACCAGCTGCAGGGTGCAGTTAAATGG
alr1706-5	TTGTAAGAATTC ACTATTACGATATAATC
alr3857-16	AGAGGTCTGCAGACCTGGTATAGCGTC
alr3857-17	TTTTGAGGTACCATTATGGCGTTTGAT

Table 1. Oligodeoxynucleotide primers used in this work. The underlined letters indicate a restriction site.

inhibitor mixture tablet (cOmplete Tablets, Mini EDTA-free; Roche) were passed through a French pressure cell (20,000 psi, three passages) followed by centrifugation at 5,000 g during 15 min. The resulting supernatant was taken as the Total extract. This was further centrifuged at 130,000 g 1 hour to give a supernatant (Soluble fraction) and a pellet, which was washed with PBS buffer (130,000 g, 30 min) and finally resuspended in 1 ml of the same buffer (Membrane fraction). Total protein was determined by a modified Lowry procedure³⁵. Aliquots of each Total extract, and Soluble and Membrane fractions (selected to give bands of intensity appropriate for scanning and quantification) were resolved in 12% SDS-PAGE gels and subjected to western blot analysis with an antibody against *Anabaena* FtsZ²⁴ or the D1 protein, an integral membrane protein of the photosystem II core.

BACTH assays. BACTH assays based on the reconstitution of adenylate cyclase from *Bordetella pertussis*³⁶ were performed with genes amplified by PCR using plasmid pCSFR22²⁴ (*ftsZ*) or *Anabaena* genomic DNA as template. The following primer pairs were used for amplification: *ftsZ*-46/*ftsZ*-45 (FtsZ-T18), *ftsZ*-34/*ftsZ*-32 (T18-FtsZ), *sepF*-18/*sepF*-21 (SepF-T18), *sepF*-18/*sepF*-17 (T18-SepF), *zipN*-21/*zipN*-22 (T25-ZipN), all1616-1/all1616-3 (Ftn6-T18), all1757-1/all1757-5 (FtsX-T18), all1757-1-/all1757-4 (T18-FtsX), alr0718-16/alr0718-17 (T18-FtsI), alr3857-16/alr3857-17 (T18-FtsQ), all0154-11/all0154-13 (T18-FtsW) and alr1706-4/alr1706-5

(T18-FtsE). The resulting PCR products, which were flanked by PstI and EcoRI ends (for *ftsZ*, *sepF*, *ftn6*, *ftsW*, *ftsX* and *ftsI*), KpnI and PstI ends (*zipN*), or HindIII and EcoRI (*ftsE*), were cloned in pUT18, pUT18C or pKT25 digested with the same enzymes, producing fusions to the 5' or 3' ends of the genes encoding the adenylate cyclase T18 and T25 fragments. All the resulting plasmids were verified by sequencing. Plasmids were transformed into *E. coli* XL1-Blue for amplification. Isolated plasmids were co-transformed into strain BTH101 (*cya-99*), and the transformants were plated on solid LB medium containing selective antibiotics and 1% glucose.

To estimate the strength of interactions, β -galactosidase activity was measured after growth of the *E. coli* strains in liquid medium in the presence of IPTG and antibiotics, using *o*-nitrophenol- β -galactoside as a substrate. The *o*-nitrophenol produced per mg of protein versus time was represented, and β -galactosidase activity was deduced from the slope of the linear function²⁴.

Microscopy. For staining with FM1-43, 2.5 μ l of the dye (0.1 mg/ml DMSO; Molecular Probes) were added to 0.1 ml of cell suspension, incubated for 10 min at room temperature and washed twice with growth medium. For staining with DAPI, 5.0 μ l of the dye (10 μ g/ml) were added to 0.1 ml of cell suspension. For immunolocalization with antibodies against *Anabaena* FtsZ or SepJ, filaments were treated as described²⁴. Samples were visualized in a Leica DM6000B fluorescence microscope and photographed with an ORCA-ER camera (Hamamatsu). Fluorescence was monitored with a FITC L5 filter (excitation band-pass, 480/40; emission band-pass, 527/30) for FM1-43 staining and immunolocalization; an A4 filter (excitation, 360/40; emission, 470/40) for DAPI staining; and a Tx2 filter (excitation, 560/40; emission, 645/75) for cyanobacterial autofluorescence. Images were treated with the Leica Application Suite Advanced Fluorescence software and with ImageJ 1.47i software (<https://imagej.nih.gov/ij>). Cell area was estimated automatically with ImageJ 1.47i processing of light-microscopy images, and the results obtained were compared to those obtained by manual estimations with fluorescence microscopy images after staining filaments with the FM1-43 dye. Nucleoid area was estimated with ImageJ processing of DAPI images. Data were plotted using the open source software RStudio Desktop (<https://www.rstudio.com/products/rstudio/>). GFP fluorescence and *Anabaena* autofluorescence were monitored with a Leica HCX PLAN-APO 63 \times 1.4 NA oil immersion objective attached to a Leica TCS SP2 confocal laser-scanning microscope. Excitation was made using 488-nm irradiation from an argon ion laser, and fluorescence was collected across windows of 500–540 nm (GFP imaging) or 630–700 nm (cyanobacterial autofluorescence). From the images of GFP fluorescence, the fluorescence intensity was plotted against the distance within each cell using the ImageJ software, and the RStudio Desktop was used for compilation into demographs.

References

- Herrero, A. & Flores E. Genetic Responses to Carbon and Nitrogen Availability in Cyanobacteria. *Environ Microbiol*, <https://doi.org/10.1111/1462-2920.14370>.
- Flores, E. & Herrero, A. Compartmentalized function through cell differentiation in filamentous cyanobacteria. *Nat Rev Microbiol* **8**, 39–50 (2010).
- Herrero, A., Stavans, J. & Flores, E. The multicellular nature of filamentous heterocyst-forming cyanobacteria. *FEMS Microbiol Rev* **40**, 831–854 (2016).
- Flores, E. *et al.* Septum-localized protein required for filament integrity and diazotrophy in the heterocyst-forming cyanobacterium *Anabaena* sp. strain PCC 7120. *J Bacteriol* **189**, 3884–3890 (2007).
- Nayar, A. S., Yamaura, H., Rajagopalan, R., Risser, D. D. & Callahan, S. M. FraG is necessary for filament integrity and heterocyst maturation in the cyanobacterium *Anabaena* sp. strain PCC 7120. *Microbiology* **153**, 601–607 (2007).
- Mullineaux, C. W. *et al.* Mechanism of intercellular molecular exchange in heterocyst-forming cyanobacteria. *EMBO J* **27**, 1299–1308 (2008).
- Flores, E., Herrero, A., Forchhammer, K. & Maldener, I. Septal junctions in filamentous heterocyst-forming cyanobacteria. *Trends Microbiol* **24**, 79–82 (2016).
- Ramos-León, F., Mariscal, V., Battchikova, N., Aro, E.-M. & Flores, E. Septal protein SepJ from the heterocyst-forming cyanobacterium *Anabaena* forms multimers and interacts with peptidoglycan. *FEBS OpenBio* **7**, 1515–1526 (2017).
- Rippka, R., Deruelles, J., Waterbury, J. B., Herdman, M. & Stanier, R. Y. Generic assignments, strain histories and properties of pure cultures of cyanobacteria. *J Gen Microbiol* **111**, 1–61 (1979).
- Duman, R. *et al.* Structural and genetic analyses reveal the protein SepF as a new membrane anchor for the Z ring. *Proc Natl Acad Sci USA* **118**, E4601–E4610 (2013).
- Meier, E. L., Razavi, S., Inoue, T. & Goley, E. D. A novel membrane anchor for FtsZ is linked to cell wall hydrolysis in *Caulobacter crescentus*. *Mol Microbiol* **101**, 265–280 (2016).
- Mosyak, L. *et al.* The bacterial cell-division protein ZipA and its interaction with an FtsZ fragment revealed by X-ray crystallography. *EMBO J* **19**, 3179–3191 (2000).
- Pichoff, S. & Lutkenhaus, J. Tethering the Z ring to the membrane through a conserved membrane targeting sequence in FtsA. *Mol Microbiol* **55**, 1722–1734 (2005).
- Rowlett, V. W. & Margolin, W. 3D-SIM super-resolution of FtsZ and its membrane tethers in *Escherichia coli* cells. *J Bacteriol* **196**, 2089–2100 (2014).
- Haeusser, D. & Margolin, W. Splitsville: structural and functional insights into the dynamic bacterial Z ring. *Nat Rev Microbiol* **14**, 305–319 (2016).
- Bisson-Filho, A. W., Hsu, Y. P., Squyres, G. R. & Kuru, E. Treadmilling by FtsZ filaments drives peptidoglycan synthesis and bacterial cell division. *Science* **355**, 739–743 (2017).
- Miyagishima, S.-Y. Y., Wolk, C. P. & Osteryoung, K. W. Identification of cyanobacterial cell division genes by comparative and mutational analyses. *Mol Microbiol* **56**, 126–143 (2005).
- Cassier-Chauvat, C. & Chauvat, F. Cell division in cyanobacteria. In: *The Cell Biology of Cyanobacteria*. Flores, E. & Herrero, A. (eds) Norfolk, UK: Caister Academic Press, pp. 7–27 (2014).
- Gündoğdu, M. E. *et al.* Large ring polymers align FtsZ polymers for normal septum formation. *EMBO J* **30**, 617–626 (2011).
- Koksharova, O. A. & Wolk, C. P. A novel gene that bears a DnaJ motif influences cyanobacterial cell division. *J Bacteriol* **184**, 5524–5528 (2002).
- Corrales-Guerrero, L. *et al.* FtsZ of filamentous, heterocyst-forming cyanobacteria has a conserved N-terminal peptide required for normal FtsZ polymerization and cell division. *Frontiers Microbiol* October 2018. Vol. 9. Article 2260 (2018).
- Mazouni, K., Domain, F. & Cassier-Chauvat, C. Molecular analysis of the key cytokinetic components of cyanobacteria: FtsZ, ZipN and MinCDE. *Mol Microbiol* **52**, 1145–1158 (2004).

23. Marbouty, M., Saguez, C., Cassier-Chauvat, C. & Chauvat, F. ZipN, an FtsA-like orchestrator of divisome assembly in the model cyanobacterium *Synechocystis* PCC6803. *Mol Microbiol* **74**, 409–420 (2009a).
24. Ramos-León, F., Mariscal, V., Frías, J. E., Flores, E. & Herrero, A. Divisome-dependent subcellular localization of cell-cell joining protein SepJ in the filamentous cyanobacterium *Anabaena*. *Mol Microbiol* **96**, 566–580 (2015).
25. Flaherty, B. L., Nieuwerburgh, F., Head, S. R. & Golden, J. W. Directional RNA deep sequencing sheds new light on the transcriptional response of *Anabaena* sp. strain PCC 7120 to combined-nitrogen deprivation. *BMC genomics* (2011).
26. Mitschke, J., Vioque, A., Haas, F., Hees, W. R. & Muro-Pastor, A. M. Dynamics of transcriptional start site selection during nitrogen stress-induced cell differentiation in *Anabaena* sp. PCC7120. *Proc Natl Acad Sci USA* **108**, 20130–20135 (2011).
27. Pulido, P. & Leister, D. Novel DNAJ-related proteins in *Arabidopsis thaliana*. *New Phytologist* **217**, 480–490 (2018).
28. Mura, A. *et al.* Roles of the essential protein FtsA in cell growth and division in *Streptococcus pneumoniae*. *J Bacteriol* **199**(3), e00608–16 (2016).
29. Koksharova, O. A., klint, J. & Rasmussen, U. Comparative proteomics of cell division mutants and wild-type of *Synechococcus* sp. strain PCC 7942. *Microbiology* **153**, 2505–2517 (2007).
30. Marbouty, M., Saguez, C. & Chauvat, F. The cyanobacterial cell division factor Ftn6 contains an N-terminal DnaD-like domain. *BMC Structural Biology* **9**, 54 (2009b).
31. Burnat, M. & Flores, E. Inactivation of agmatinase expressed in vegetative cells alters arginine catabolism and prevents diazotrophic growth in the heterocyst-forming cyanobacterium *Anabaena*. *MicrobiologyOpen* **3**(5), 777–792 (2014).
32. Elhai, J., Vepritskiy, A., Muro-Pastor, A. M., Flores, E. & Wolk, C. P. Reduction of conjugal transfer efficiency by three restriction activities of *Anabaena* sp. strain PCC 7120. *J Bacteriol* **179**, 1998–2005 (1997).
33. Black, T. A., Cai, Y. & Wolk, C. P. Spatial expression and autoregulation of *hetR*, a gene involved in the control of heterocyst development in *Anabaena*. *Mol Microbiol* **9**, 77–84 (1993).
34. Merino-Puerto, V., Mariscal, V., Mullineaux, C. W., Herrero, A. & Flores, E. Fra proteins influencing filament integrity, diazotrophy and localization of septal protein SepJ in the heterocyst-forming cyanobacterium *Anabaena* sp. *Mol Microbiol* **75**, 1159–1170 (2010).
35. Markwell, M. A. K., Haas, S. M., Bieber, L. L. & Tolbert, N. E. A modification of the Lowry procedure to simplify protein determination in membrane and lipoprotein samples. *Anal Biochem* **87**, 206–210 (1978).
36. Karimova, G., Dautin, N. & Ladant, D. Interaction network among *Escherichia coli* membrane proteins involved in cell division as revealed by bacterial two-hybrid analysis. *J. Bacteriol* **187**, 2233–2243 (2005).
37. Sapai, N., Guerneur, Y. & Deléage, G. Prediction of amphiphatic in-plane membrane anchors in monotopic proteins using a SVM classifier. *BMC Bioinformatics* **7**, 255 (2006).

Acknowledgements

Work was supported by grants BFU2013-44686-P and BFU2016-77097-P from Agencia Estatal de Investigación, Spain, cofinanced by the European Regional Development Fund (EU). We thank Anna Marika Lindall (CSIC, Sevilla) for antibodies against D1, and Enrique Flores (CSIC, Sevilla) for suggestions and critical reading of the manuscript.

Author Contributions

All authors designed the research and analyzed and discussed data; S.C., S.P., L.C., A.V. and S.A. performed the experiments; and A.H. directed the research, wrote the paper and drew Figure 11.

Additional Information

Competing Interests: The authors declare no competing interests.

Publisher's note: Springer Nature remains neutral with regard to jurisdictional claims in published maps and institutional affiliations.



Open Access This article is licensed under a Creative Commons Attribution 4.0 International License, which permits use, sharing, adaptation, distribution and reproduction in any medium or format, as long as you give appropriate credit to the original author(s) and the source, provide a link to the Creative Commons license, and indicate if changes were made. The images or other third party material in this article are included in the article's Creative Commons license, unless indicated otherwise in a credit line to the material. If material is not included in the article's Creative Commons license and your intended use is not permitted by statutory regulation or exceeds the permitted use, you will need to obtain permission directly from the copyright holder. To view a copy of this license, visit <http://creativecommons.org/licenses/by/4.0/>.

© The Author(s) 2019